ISSN 1070-4280, Russian Journal of Organic Chemistry, 2022, Vol. 58, No. 12, pp. 1786–1796. © Pleiades Publishing, Ltd., 2022.

Three-Component Synthesis and Crystal Structure of 2-Amino-3-cyano-4*H*-pyran and -thiopyran Derivatives

I. V. Dyachenko[a], V. D. Dyachenko[a], P. V. Dorovatovskii[b], V. N. Khrustalev[c,d], D. G. Rivera[e], and V. G. Nenajdenko[f,*]

[a] *Lugansk State Pedagogical University, Lugansk, 91011 Ukraine*

[b] *"Kurchatovskii Institute" National Research Center, Moscow, 123182 Russia*

[c] *Peoples' Friendship University of Russia, Moscow, 117198 Russia*

[d] *Zelinsky Institute of Organic Chemistry, Russian Academy of Sciences, Moscow, 119991 Russia*

[e] *University of Havana, Havana, 10400 Cuba*

[f] *Faculty of Chemistry, Moscow State University, Moscow, 119991 Russia*

**e-mail: nenajdenko@gmail.com*

Received May 25, 2022; revised June 10, 2022; accepted June 12, 2022

Abstract—2-Amino-3-cyano-4*H*-pyran and -thiopyran derivatives were synthesized by three-component reactions of aldehydes, dimedone, and CH acids. The molecular and crystal structures of the synthesized compounds were determined by X-ray analysis.

Keywords: three-component reaction, dimedone, malononitrile, cyanothioacetamide, selenoamide, 4*H*-pyran, thiopyran, furan, X-ray analysis

DOI: 10.1134/S1070428022120077

INTRODUCTION

2-Amino-3-cyano-4*H*-pyran derivatives are known to exhibit pronounced biological activity; in particular, they inhibit SARS-CoV-2 [1], cholinesterase [2], *Staphylococcus aureus* [3, 4], tumors [5–7], acetylcholinesterase [8], and *M. tuberculosis* [9]. They also show antioxidant [10–12] and anti-inflammatory [13–15] activities.

RESULTS AND DISCUSSION

Taking into account practical importance of substituted 2-amino-3-cyano-4*H*-pyrans, we continued our research in the field of chemistry of these organic compounds [16–20] and studied three-component condensation of dimedone (**1**), malononitrile (**2**) and benzaldehyde (**3a**) or 3-phenylpropanal (**3b**) in 2-aminoethanol at 20°C. As a result, tetrahydrochromene derivatives **4a** and **4b** were obtained. A probable reaction mechanism (Scheme 1) involves Knoevenagel condensation of aldehyde **3** and malononitrile (**2**) with the formation of intermediate **A**, followed by Michael addition of dimedone (**1**). Intramolecular cyclization of adduct **B** yields 81–88% of final product **4**. In this reaction, 2-aminoethanol is likely to act as a base catalyst. Compounds **4** were synthesized previously in the presence of piperidine [21] or morpholine [22].

Treatment of pyran **4a** with bromine in methanol under irradiation with a 500-W lamp led to the formation of benzofuran derivative **5** in 45% yield. Presumably, in the first stage conjugate addition of bromine and methanol to the double $C^{4a}=C^{8a}$ bond gives intermediate **C**, and next follows bromination of the second double C=C bond to produces 3,4a-dibromo derivative **D**. Opening of the pyran ring in **D** leads to intermediate **E** which undergoes cyclization to final structure **5** with elimination of ammonium bromide (Scheme 1). It should be noted that pyran derivatives structurally related to **4** reacted with bromine in methanol through opening of the heteroring to give methyl 2-cyano-3-(4,4-dimethyl-2,6-dioxocyclohexyl)-3-(4-hydroxyphenyl)prop-2-enoate [23], 3-aryl-3-(2-hydroxy-4,4-dimethyl-6-oxocyclohex-1-en-1-yl)-propionic acids were obtained by the action of sulfuric

Scheme 1.

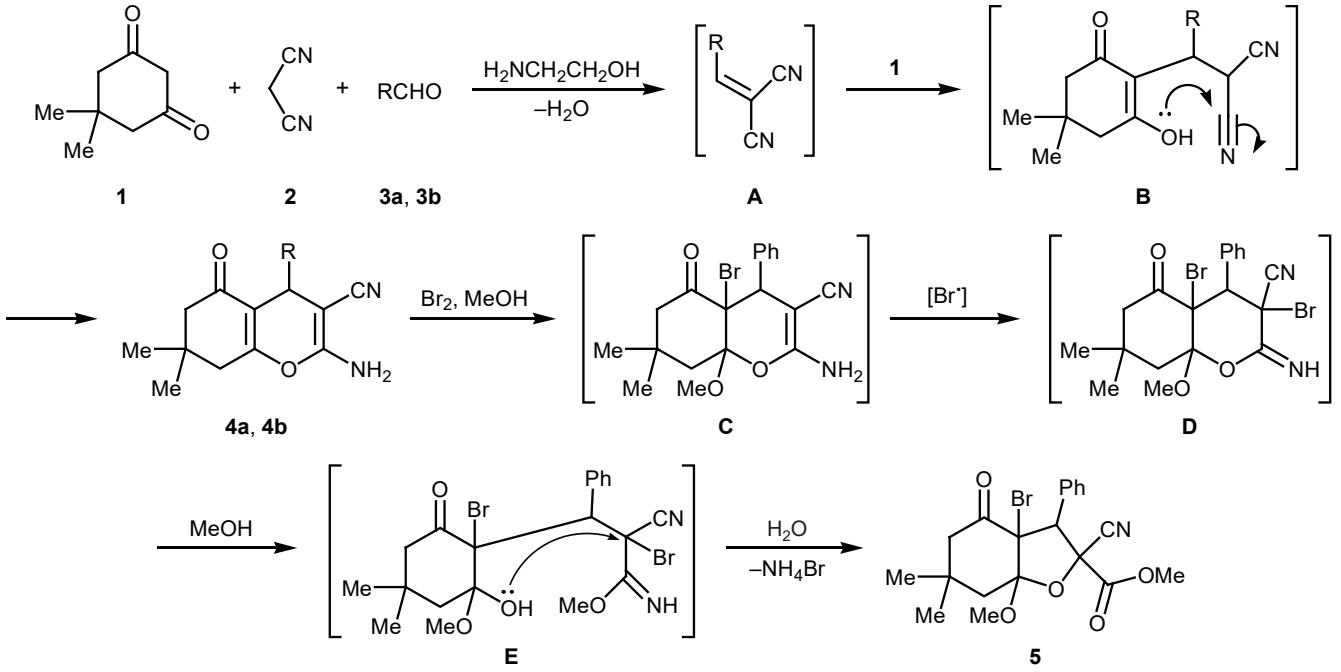

R = Ph (**a**), $PhCH_2CH_2$ (**b**).

acid and boiling formic acid [24], and their oxidation with 1-chloropyrrolidine-2,5-dione, iodine, sodium chlorate, or sodium hypochlorite produced alkyl 3-aryl-6,6-dimethyl-4-oxooctahydrobenzofuran-2-carboxylates [25].

A similar three-component condensation of dimedone (**1**), 4-chlorobenzaldehyde (**6**), and methyl 3-amino-3-selanylidenepropanoate (**7**) afforded chromene **8**. The reaction was carried out in anhydrous ethanol at 20°C under argon in the presence of an equimolar amount of *N*-methylmorpholine. Assumingly, the first stage of this process is Knoevenagel condensation of **6** and **7** to form intermediate **F**, which is followed by Michael addition of CH acid **1**. Chemoselective cyclization of adduct **G** thus formed with elimination of hydrogen selenide yields final product **8** (Scheme 2).

Unexpected result was obtained in the three-component condensation of dimedone (**1**), cyanothioacetamide (**9**), and cyclohex-3-ene-1-carbaldehyde (**10**) in

Scheme 2.

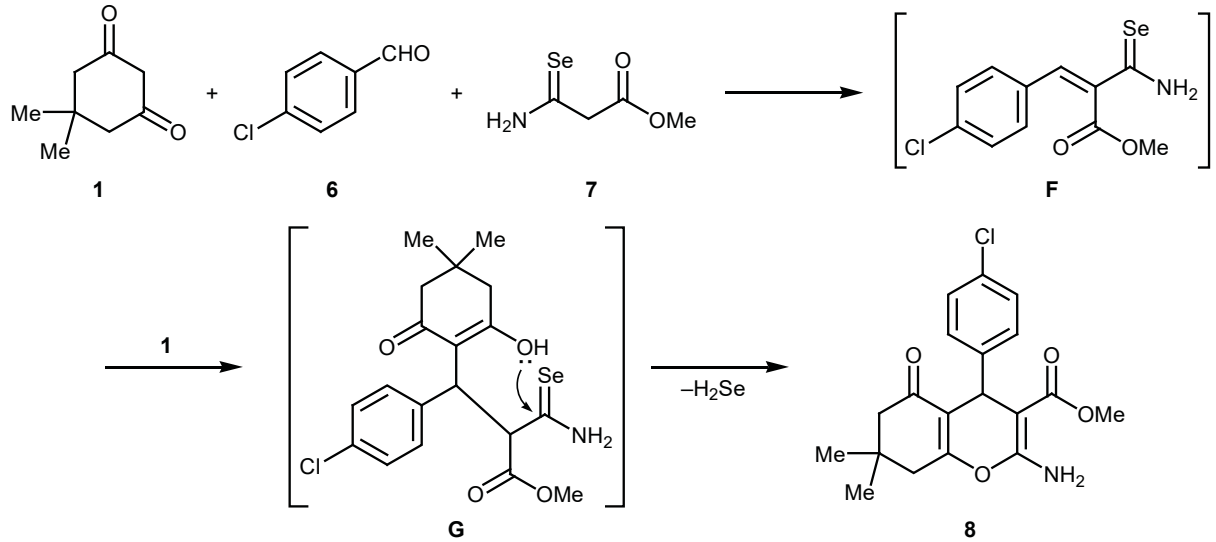

Scheme 3.

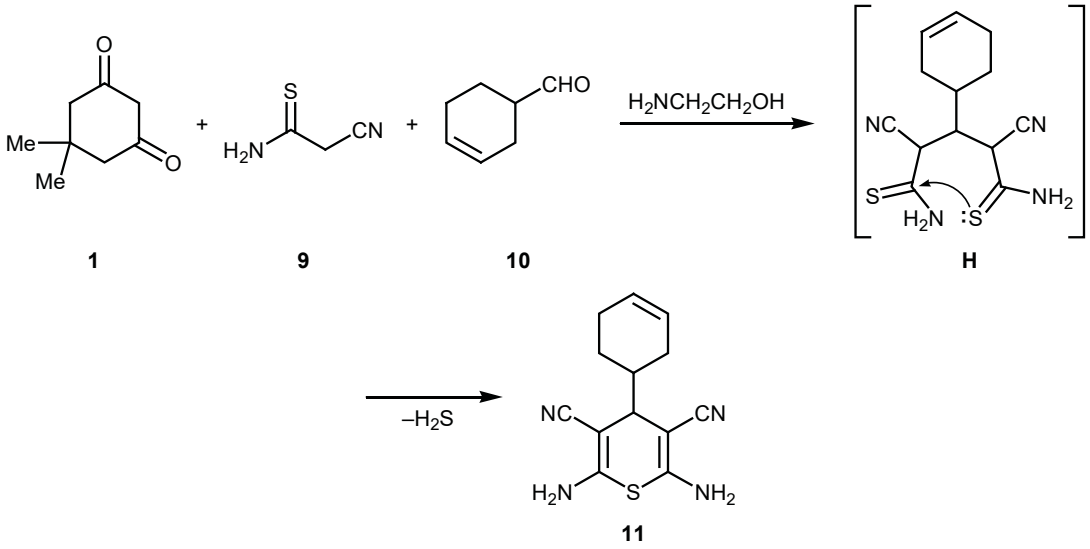

1 **9** **10** **H** **11**

2-aminoethanol at 20°C. The product of this reaction was 4*H*-thiopyran derivative **11**. This may be explained assuming that the Michael addition stage involves the second molecule of CH acid **9** instead of dimedone (**1**); the subsequent chemoselective intramolecular cyclization of intermediate **H** gives thiopyran **11**. The maximum yield of **11** was achieved using reactants **9** and **10** at a ratio of 2:1, which confirmed the proposed scheme (Scheme 3). Compound **11** was synthesized by us previously by the reaction of malononitrile (**2**) with cyanothioacetamide (**9**) and aldehyde **10** in ethanol in the presence of morpholine [26].

The structure of compounds **4a**, **4b**, **5**, **8**, and **11** was confirmed by their spectral characteristics. The IR spectra of **4a**, **4b**, **5**, **8**, and **11** showed absorption bands typical of stretching vibrations of functional groups present in their molecules, and their ^{1}H and ^{13}C NMR spectra were consistent with the assigned structures (see Experimental). Furthermore, the molecular and crystal structures of compounds **4b**, **5**, **8**, and **11** were determined by X-ray analysis.

Figure 1 shows the molecular and crystal structure of compound **4b**. The 4*H*-pyran ring of the bicyclic chromene fragment of molecule **4b** adopts a strongly

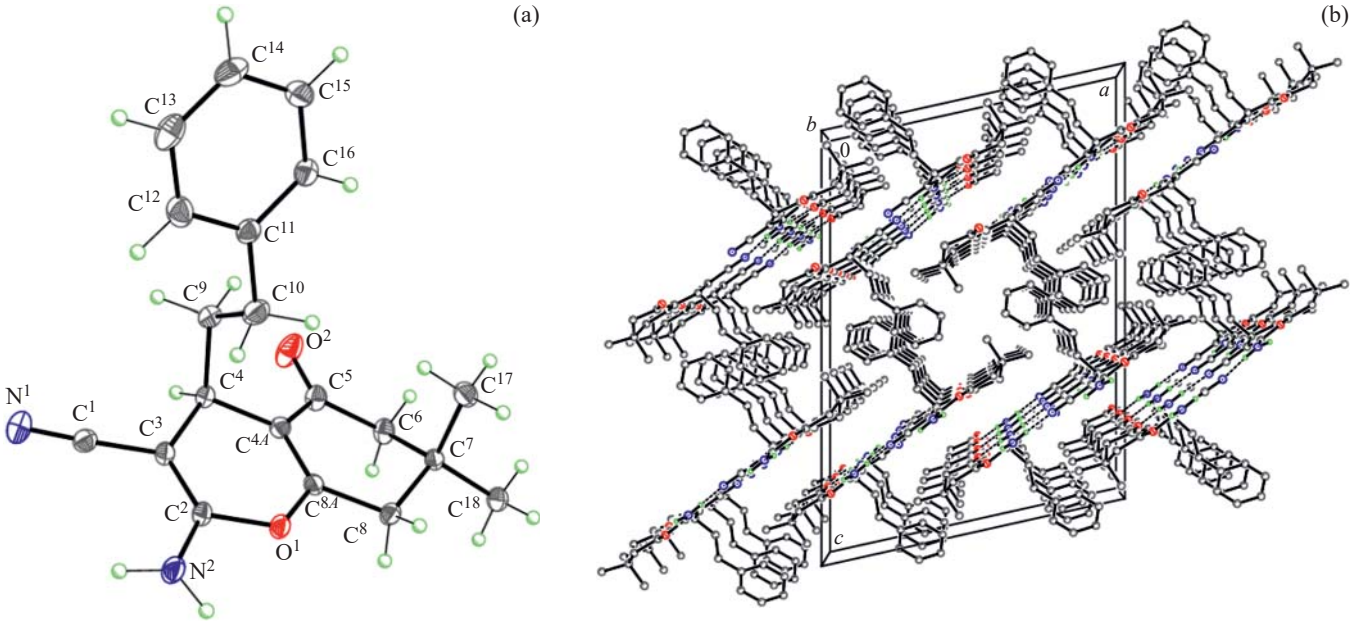

Fig. 1. (a) Molecular structure of compound **4b** and (b) packing of its molecules in crystal with the formation of H-bonded bands along the [010] direction. Intermolecular hydrogen bonds are shown with dashed lines.

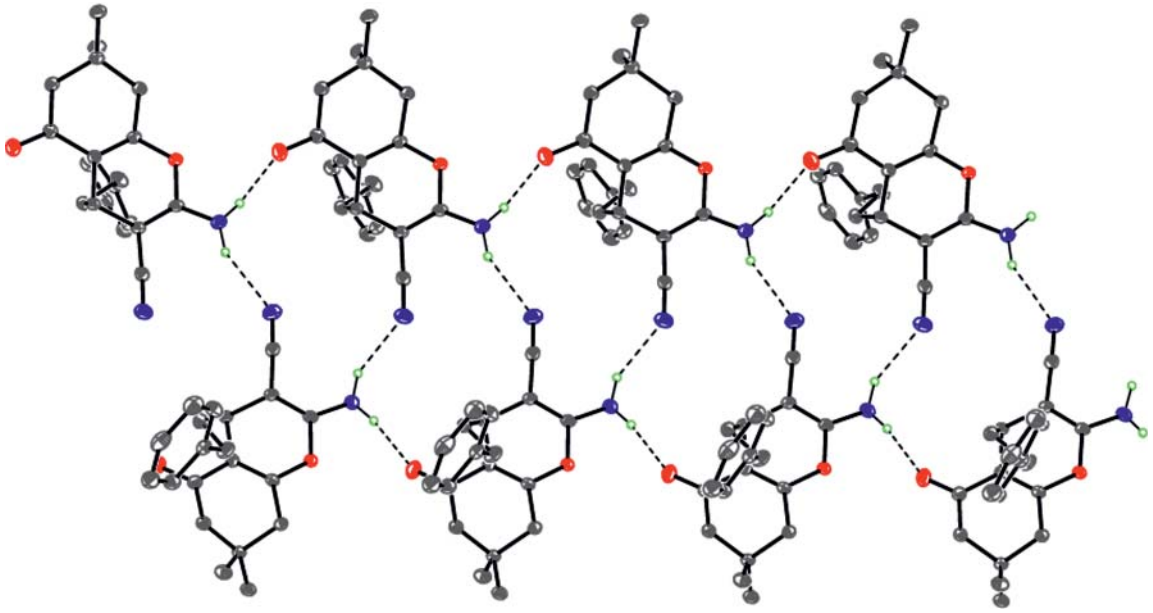

Fig. 2. Hydrogen-bonded band formed by molecules **4b** in crystal. Intermolecular hydrogen bonds are shown with dashed lines.

flattened *boat* conformation with the O^1 and C^4 atoms deviating by 0.092(2) and 0.208(2) Å, respectively, from the basal plane passing through the other ring carbon atoms. The cyclohexene ring of the chromene fragment has an unsymmetrical half-*boat* conformation with the C^7 and C^8 atoms deviating by 0.752(3) and 0.187(3) Å, respectively, from the basal plane passing through the other ring carbon atoms. The ethylene bridge connecting the benzene and pyran rings has *trans* configuration with the torsion angle $C^4C^9C^{10}C^{11}$ equal to –169.47(13)°, and it occupies less sterically favorable pseudo-*axial* position with a dihedral angle of 63.41(7)° between the benzene ring plane and basal plane of the pyran ring. The N^2 atom has trigonal–planar configuration with the sum of the bond angles equal to 359(5)°.

Molecule **4b** possesses an asymmetric carbon atom (C^4), and compound **4b** crystallizes as a racemate. Molecules **4b** in crystal are linked through fairly strong intermolecular N–H···N and N–H···O bonds (Table 1,

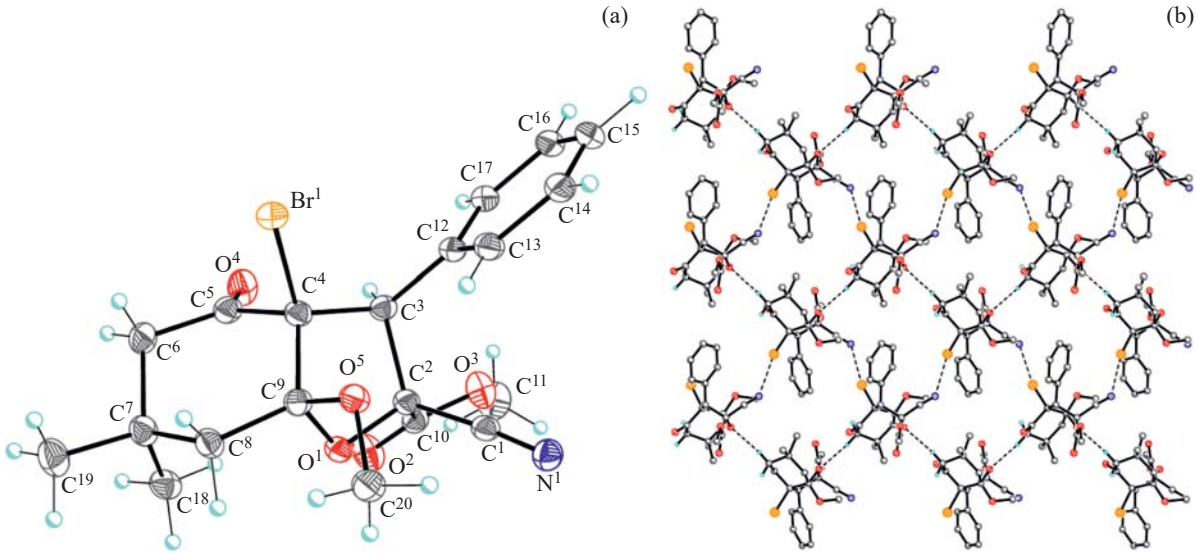

Fig. 3. (a) Molecular structure of compound **5** represented by anisotropic displacement ellipsoids for non-hydrogen atoms with a probability of 50% and (b) puckered layer formed by molecules **5** in crystal. Intermolecular hydrogen bonds C–H···O and non-covalent interactions Br···N are shown with dashed lines.

Table 1. Hydrogen bonds in the crystal structures of compounds **4b**, **5**, **8**, and **11**

D–H···A	*d*(D–H), Å	*d*(H···A), Å	*d*(D···A), Å	Angle DHA, deg
Compound **4b**				
N^2–H^{2A}···$N^{1\,a}$	0.92(2)	2.25(2)	3.101(2)	153.8(18)
N^2–H^{2B}···$O^{2\,b}$	0.89(2)	1.98(2)	2.8528(19)	169.2(19)
Compound **5**				
C^6–H^{6A}···$O^{1\,c}$	0.99	2.50	3.487(3)	173
Compound **8**				
N^1–H^{1A}···O^2	0.897(18)	2.069(18)	2.6930(16)	125.8(14)
N^1–H^{1A}···$O^{2\,d}$	0.897(18)	2.164(18)	2.9579(15)	147.2(15)
N^1–H^{1B}···$Cl^{1\,b}$	0.850(18)	2.927(18)	3.7347(13)	159.4(15)
C^9–H^{9A}···$O^{4\,e}$	0.98	2.44	3.3882(17)	164
Compound **11**				
N^1–H^{1A}···$N^{3\,f}$	0.90	2.22	3.118(3)	176
N^1–H^{1B}···$N^{2\,b}$	0.90	2.53	3.229(3)	135
N^4–H^{4A}···$N^{2\,g}$	0.90	2.12	2.995(3)	165
N^4–H^{4B}···$N^{3\,b}$	0.90	2.30	3.150(3)	157

Symmetry operations: [a] $-x + 1/2, y + 1/2, -z + 3/2$; [b] $x, y + 1, z$; [c] $-x + 3/2, y + 1/2, -z + 1/2$; [d] $-x + 2, -y + 2, -z + 1$; [e] $-x + 1, -y + 1, -z + 1$; [f] $x + 1/2, -y + 1/2, z + 1/2$; [g] $x - 1/2, -y + 1/2, z - 1/2$.

Fig. 2) to form bands along the *b* crystallographic axis. The bands are located at van der Waals distances from each other.

The molecular structure of compound **5** with atom numbering is shown in Fig. 3. The cyclohexane and tetrahydrofuran rings of the central octahydrobenzofuran fragment appear as typical slightly distorted *chair* (basal plane $C^4C^5C^7C^8$) and *envelope* conformations (basal plane $O^1C^2C^3C^4$), respectively. The six- and five-membered rings are *cis*-fused with a dihedral

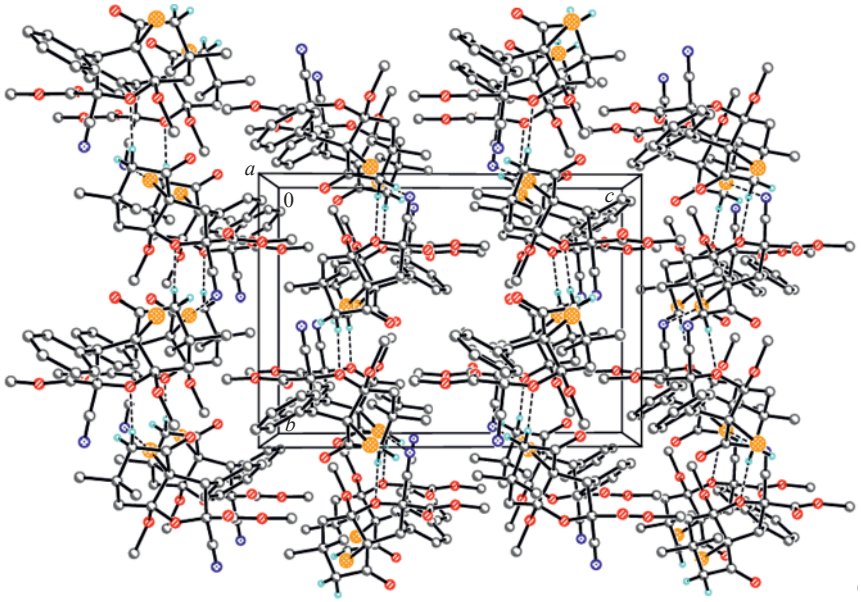

Fig. 4. Crystal structure of compound **5** represented by puckered layers parallel to the (001) plane. Intermolecular hydrogen bonds C–H···O and noncovalent interactions Br···N are shown with dashed lines.

angle of 70.60(2)° between the corresponding basal planes. Molecule **5** possesses four asymmetric carbon atoms, C^2, C^3, C^4, and C^9, and compound **5** in crystal is a racemate with 2*SR*,3*SR*,4*RS*,9*RS* relative configuration of the chiral centers. Molecules **5** in crystal are linked through weak intermolecular hydrogen bonds C–H···O (Table 1) and noncovalent interactions $Br^1\cdots N^1$ [0.5 – *x*, 0.5 + *y*, 0.5 – *z*; 3.097(3) Å] (Fig. 3b) to form puckered layers parallel to the (001) plane and arranged at van der Waals distances from each other (Fig. 4).

Figure 5a shows the molecular structure of compound **8** with atom numbering. Its structure is very similar to the structure of **4b**. The pyran ring of the chromene fragment adopts a strongly flattened *boat* conformation with the O^1 and C^4 atoms deviating by 0.089(2) and 0.181(2) Å, respectively, from the basal plane passing through the other ring carbon atoms. The cyclohexene ring has an unsymmetrical half-*boat* conformation in which the C^7 and C^8 atoms deviate by 0.706(3) and 0.121(3) Å, respectively, from the basal plane formed by the other ring atoms. The 4-chlorophenyl substituent appears in the less sterically favorable pseudo-*axial* orientation and is turned through a dihedral angle of 77.45(5)° with respect to the basal plane of the pyran ring. The acetyl group is almost coplanar to the basal plane of the pyran ring [the corresponding dihedral angle is 6.50(13)°], and its orientation is stabilized by the intramolecular hydrogen bond N–H···O (Table 1). The N^1 atom has trigonal–planar configuration with the sum of the bond angles equal to 359(4)°. Like molecule **4b**, the C^4 atom of **8** is asymmetric, and crystalline compound **8** is a racemate. However, unlike **4b**, molecules **8** in crystal are linked through intermolecular hydrogen bonds N–H···Cl, N–H···O, and C–H···O to form double-deck layers parallel to the (001) plane (Table 1, Fig. 5b). The layers give rise to a three-dimensional network through Cl···Cl noncovalent interactions with a distance of 3.4432(7) Å.

The molecular structure of 4*H*-thiopyran derivative **11** is shown in Fig. 6a. The central 4*H*-thiopyran ring has a *boat* conformation with the S^1 and C^4 atoms deviating by 0.435(4) and 0.505(4) Å, respectively, from the basal plane passed through the other ring atoms. The cyclohexenyl substituent occupies less sterically favorable axial position. The N^1 amino nitrogen atom has trigonal–planar configuration with the sum of the bond angles equal to 359.3°, whereas the N^4 atom is trigonal–pyramidal (sum of the bond angles 352.6°). The C^4 atom is asymmetric, and compound **11** in crystal is a racemate. Molecules **11** in crystal are linked through intermolecular hydrogen bonds N–H···N to form layers parallel to the (101) plane (Table 1, Fig. 6b). The layers appear at van der Waals distances from each other and form a zipper type packing (Fig. 6c).

EXPERIMENTAL

The IR spectra were recorded on a Varian Vertex 70 spectrometer from samples prepared as KBr discs. The ^1H and ^{13}C NMR spectra were recorded on a Varian VXR–400 spectrometer at 399.97 and 100 MHz, respectively, using DMSO-d_6 as solvent and tetramethylsilane as internal standard. The mass spectra

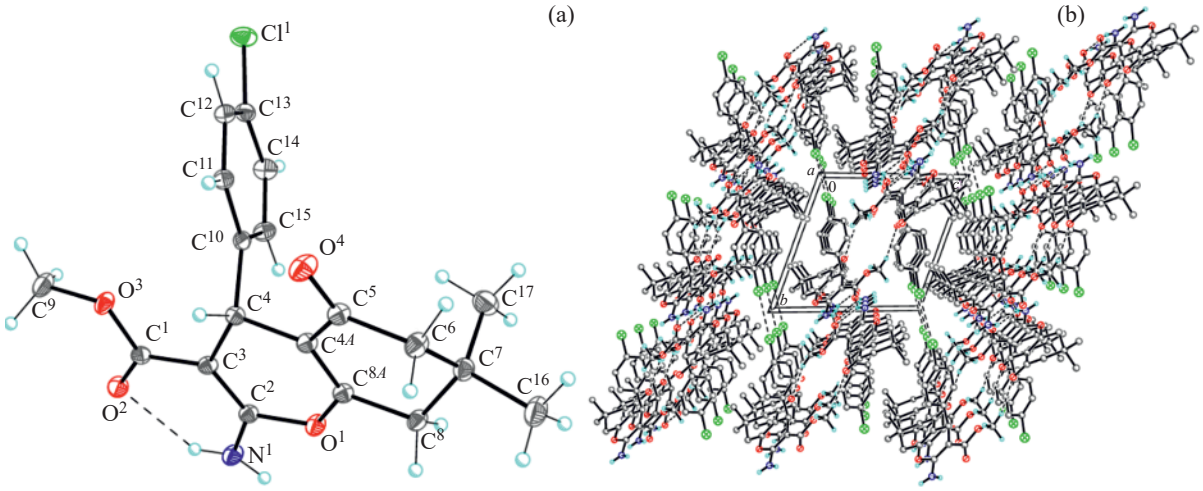

Fig. 5. (a) Molecular structure of compound **8** represented by anisotropic displacement ellipsoids for non-hydrogen atoms with a probability of 50% and (b) double-deck layer parallel to the (001) plane in the crystal structure of **8**. Intermolecular hydrogen bonds and Cl···Cl noncovalent interactions are shown with dashed lines.

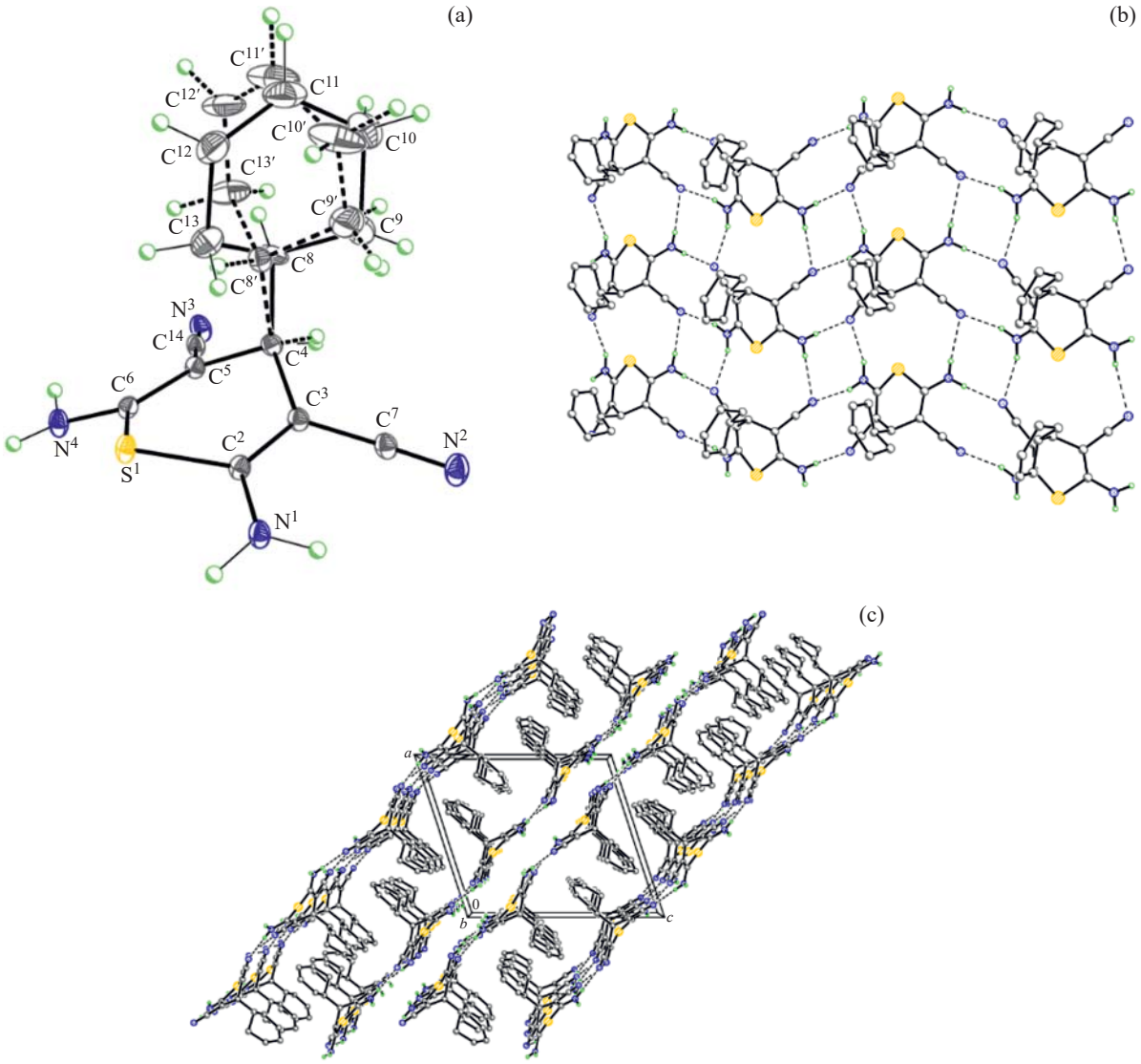

Fig. 6. (a) Molecular structure of compound **11** represented by anisotropic displacement ellipsoids for non-hydrogen atoms with a probability of 50%; alternative position of the disordered cyclohexenyl substituent is shown with dashed lines; (b) structure of a layer formed by molecules **11** in crystal; (c) zipper packing of hydrogen-bonded layers parallel to the (101) plane in the crystal structure of **11**. Intermolecular hydrogen bonds N–H···N are shown with dashed lines.

were obtained with an Orbitrap Elite high-resolution mass spectrometer; samples were dissolved in 1 mL of DMSO, and the solution was diluted with 100 volumes of 1% formic acid in acetonitrile and introduced into electrospray ionization source at a flow rate of 40 μL/min using a syringe pump; the source gas supply was turned off; needle voltage 3.5 kV, capillary temperature 275°C; positive and negative ions were detected using an orbital trap with a resolution of 480000. $[2DMSO + H]^+$ (*m*/*z* 157.03515) and dodecyl sulfate anion (*m*/*z* 265.14789) were used as internal calibrants for positive and negative ions, respectively. Elemental analysis was performed with a Perkin Elmer CHN analyzer. The melting point were measured using a Kofler hot stage. The progress of reactions and the purity of the isolated compounds were monitored by TLC on Silufol UV-254 plates using acetone–hexane (3:5) as eluent; visualization was done by treatment with iodine vapor and under UV light.

The unit cell parameters and X-ray reflection intensities for single crystals of compounds **4b**, **8**, and **11** were determined on a Bruker D8 QUEST PHOTON-III CCD diffractometer (graphite monochromator, φ- and ω-scanning). The data were processed using SAINT [27]. A correction for absorption was applied by SADABS [28]. The X-ray diffraction data for com-

Table 2. Crystallographic data for compounds **4b**, **5**, **8**, and **11**

Parameter	**4b**	**5**	**8**	**11**
Formula	$C_{20}H_{22}N_2O_2$	$C_{20}H_{22}BrNO_5$	$C_{19}H_{20}ClNO_4$	$C_{13}H_{14}N_4S$
Molecular weight	322.40	436.29	361.81	258.34
λ, Å	0.71073	0.79313	0.71073	0.71073
Temperature, K	100(2)	100(2)	100(2)	100(2)
Single crystal dimensions, mm	0.12×0.15×0.15	0.15×0.15×0.20	0.12×0.15×0.15	0.09×0.12×0.15
Crystal system	Monoclinic	Monoclinic	Triclinic	Monoclinic
Space group	*C*2/*c*	$P2_1/n$	*P*-1	$P2_1/n$
a, Å	17.9068(7)	10.462(2)	8.4306(7)	13.1978(12)
b, Å	7.7842(3)	11.383(2)	10.3027(9)	6.6851(6)
c, Å	25.0934(10)	16.001(3)	11.1579(10)	15.2544(14)
α, deg	90	90	108.614(2)	90
β, deg	102.5820(10)	92.75(3)	107.192(2)	108.248(3)
γ, deg	90	90	91.954(2)	90
V, Å^3	3413.8(2)	1903.4(6)	868.54(13)	1278.2(2)
Z	8	4	2	4
d_{calc}, g/cm^3	1.255	1.523	1.383	1.342
F(000)	1376	896	380	544
μ	0.082	2.865	0.244	0.241
2θ range, deg	2.87–32.63	2.45–31.00	2.70–32.66	2.46–30.63
Total number of reflections	30093	21259	14998	19149
Number of independent reflections, R_{int}	6228, 0.107	4338, 0.044	6327, 0.040	3891, 0.098
Number of reflections with $I > 2\sigma(I)$	3701	3978	4654	2586
Number of refined parameters	225	248	235	217
R_1 [$I > 2\sigma(I)$]	0.060	0.044	0.045	0.072
wR_2 (all independent reflections)	0.143	0.106	0.110	0.192
Goodness of fit with respect to F^2	1.037	1.032	1.045	1.027
T_{min}; T_{max}	0.975; 0.987	0.561; 0.636	0.954; 0.963	0.959; 0.972
Extinction coefficient	–	0.0072(7)	–	–
$\Delta\rho_{max}$; $\Delta\rho_{min}$, $\bar{e}$ Å^{-3}	0.350; –0.321	0.656; –0.949	0.422; –0.339	0.680; –0.366

pound **5** were obtained at the "Kurchatov Institute" National Research Center on an *RSA* synchrotron station equipped with a two-coordinate Rayonix SX165 CCD detector (φ-scanning with a step of 1.0°). The data were processed using iMOSFLM program implemented in CCP4 software package [29]. Absorption of X-ray radiation was taken into account using SCALA program [30]. The principal crystallographic data and refinement parameters are collected in Table 2.

The structures were determined by direct methods and were refined against F^2 by the full-matrix least-squares method in anisotropic approximation for non-hydrogen atoms. The cyclohexene ring in molecule **11** was disordered by two positions with different populations. Hydrogen atoms of the amino groups of

4b and **8** were localized objectively by difference Fourier syntheses and were refined isotropically with fixed thermal displacement parameters [U_{iso}(H) = 1.2U_{eq}(N)]. Hydrogen atoms of the amino groups of **11** were localized objectively by difference Fourier syntheses and were refined with fixed positional parameters (riding model) and isotropic thermal displacement parameters [U_{iso}(H) = 1.2U_{eq}(N)]. The positions of the other hydrogens were calculated geometrically and refined with fixed positional parameters (riding model) and isotropic thermal displacement parameters [U_{iso}(H) = 1.5U_{eq}(C) for methyl groups and 1.2U_{eq}(C) for other groups]. All calculations were performed using SHELXTL [31]. The tabulated coordinates of atoms, bond lengths, bond and torsion angles, and anisotropic displacement parameters for compounds **4b**, **5**, **8**, and **11** were deposited to the Cambridge Crystallographic Data Centre (CCDC entry nos. 2143982, 2143983, 2143984, and 2143985, respectively).

2-Amino-7,7-dimethyl-5-oxo-4-phenyl-5,6,7,8-tetrahydro-4*H*-chromene-3-carbonitrile (4a). A mixture of 1.0 mL (10 mmol) of benzaldehyde (**3a**) and 0.66 g (10 mmol) of malononitrile (**2**) in 15 mL of 2-aminoetanol was stirred at 20°C for 25 min, 1.4 g (10 mmol) of dimedone (**1**) was added, and the mixture was stirred for 25 min and left to stand for 48 h. The mixture was diluted with an equal volume of water, and the precipitate was filtered off and washed with water, ethanol, and hexane. Yield 3.6 g (88%), colorless crystals, mp 238–240°C (from EtOH); published data [21]: mp 237–238°C.

2-Amino-7,7-dimethyl-5-oxo-4-(2-phenylethyl)-5,6,7,8-tetrahydro-4*H*-chromene-3-carbonitrile (4b) was synthesized in a similar from 1.34 g of 3-phenylpropanal (**3b**). Yield 2.6 g (81%), colorless crystals, mp 197–198°C (from EtOH); published data [22]: mp 199–200°C. ^{13}C NMR spectrum, δ_C, ppm: 23.2, 24.5, 25.5, 26.8, 27.9, 32.3, 46.3, 51.2, 108.5, 116.3, 121.9 (2C), 124.4 (2C), 124.6 (2C), 137.9, 156.2, 159.5, 192.6. Mass spectrum (ESI): *m*/*z* 323.1759 [*M* + H]$^+$. $C_{20}H_{22}N_2O_2$. Calculated: *M* + H 323.1681.

Methyl 3a-bromo-2,7a-dimethoxy-6,6-dimethyl-4-oxo-3-phenyloctahydro-1-benzofuran-2-carboxylate (5). Molecular bromine, 0.51 mL (10 mmol), was added dropwise at room temperature to a mixture of 2.94 g (10 mmol) of pyran **4a** and 30 mL under stirring on a magnetic stirrer and irradiation with a 500-W lamp. The rate of the addition was maintained so that the reaction mixture retained pink color (~15 min). The mixture was then stirred for 60 min and left to stand in a refrigerator. After 24 h, the mixture was diluted with an equal volume of water and left to stand further for 24 h at room temperature. The colorless needles were filtered off and successively washed with water, methanol, and hexane. Yield 1.9 g (45%), mp 208–210°C. IR spectrum, ν, cm^{-1}: 2245 (C≡N), 1715 (C=O), 1702 (C=O). ^{1}H NMR spectrum, δ, ppm (*J*, Hz): 1.01 s (3H, Me), 1.12 s (3H, Me), 2.06 d (1H, CH_2, ^2J = 14.8 Hz), 2.25 d (1H, CH_2, ^2J = 14.8 Hz), 3.21 d (1H, CH_2, ^2J = 17.8 Hz), 3.27 d (1H, CH_2, ^2J = 17.8 Hz), 3.50 s (3H, MeO), 3.84 s (3H, OMe), 4.95 s (1H, 3-H), 7.28–7.41 m (3H, H_{arom}), 7.53–7.62 m (2H, H_{arom}). ^{13}C NMR spectrum, δ_C, ppm: 26.1, 32.2, 32.7, 48.5, 50.2, 54.3, 55.1, 66.2, 80.04, 111.6, 115.5, 128.4 (2C), 129.2, 133.0 (2C), 135.2, 165.4, 199.2, 207.5. Mass spectrum (ESI): *m*/*z* 437.0681 [*M* + H]$^+$. $C_{20}H_{22}BrNO_5$. Calculated: *M* + H 437.0597.

Methyl 2-amino-4-(4-chlorophenyl)-7,7-dimethyl-5-oxo-5,6,7,8-tetrahydro-4*H*-chromene-3-carboxylate (8). To a mixture of 1.4 g (10 mmol) of 4-chlorobenzaldehyde (**6**) and 20 mL of anhydrous ethanol we added with stirring at 20°C under argon 1.81 g (10 mmol) of CH acid **7** and 1.1 mL (10 mmol) of *N*-methylmorpholine. The mixture was stirred for 30 min, 1.4 g (10 mmol) of dimedone (**1**) was added, and the mixture was stirred for 1 h and left to stand for 24 h. The precipitate was filtered off and washed with ethanol and hexane. Yield 2.8 g (78%), colorless cubic crystals, mp 173–175°C (from EtOH). IR spectrum, ν, cm^{-1}: 3408, 3345, 3241 (NH_2), 1696, 1713 (C=O), 1649 (δNH_2). ^{1}H NMR spectrum, δ, ppm (*J*, Hz): 0.85 s (3H, Me), 1.00 s (3H, Me), 2.03 d (1H, CH_2, ^2J = 16.1 Hz), 2.23 d (1H, CH_2, ^2J = 16.1 Hz), 2.45 d (1H, CH_2, ^2J = 17.6 Hz), 2.47 d (1H, CH_2, ^2J = 17.6 Hz), 3.47 s (3H, MeO), 4.48 s (1H, 4-H), 7.10 d (2H, H_{arom}, *J* = 8.4 Hz), 7.23 d (2H, H_{arom}, *J* = 8.4 Hz), 7.59 br.s (2H, NH_2). ^{13}C NMR spectrum, δ_C, ppm: 26.9, 29.1, 32.3, 33.3, 50.3, 51.0, 77.6, 115.6, 128.2 (2C), 128.6, 129.8, 130.8 (2C), 145.8, 159.7, 162.7, 168.6, 196.2. Mass spectrum (ESI): *m*/*z* 362.1162 [*M* + H]$^+$. $C_{19}H_{20}ClNO_4$. Calculated: *M* + H 362.1081.

2,6-Diamino-4-(cyclohex-3-en-1-yl)-4*H*-thiopyran-3,5-dicarbonitrile (11). Cyanothioacetamide (**9**, 2.0 g, 20 mmol) was added with stirring at 20°C to a solution of 0.94 mL (10 mmol) of aldehyde **10** in 15 mL of 2-aminoethanol, and the mixture was stirred for 2 h and left to stand for 24 h. The mixture was diluted with an equal volume of water, and the precipitate was

successively washed with water, ethanol, and hexane. Yield 1.83 g (71%), yellow crystals, mp 199–201°C (from AcOH) [26]. ^{13}C NMR spectrum, δ_C, ppm: 25.1, 26.3, 29.0, 44.5, 70.7, 71.1, 120.2, 126.2 (2C), 127.1 (2C), 153.2, 153.3. Mass spectrum (ESI): *m*/*z* 259.1012 $[M + H]^+$. $C_{13}H_{14}N_4S$. Calculated: M + H 259.0939.

CONCLUSIONS

The condensation of dimedone, malononitrile, and aldehydes in 2-aminoethanol afforded pyran derivatives whose molecular and crystal structures were determined by X-ray analysis. Radical bromination of 2-amino-7,7-dimethyl-5-oxo-4-phenyl-5,6,7,8-tetrahydro-4*H*-chromene-3-carbonitrile in methanol was accompanied by pyran ring contraction with the formation of benzofuran derivative.

AUTHOR INFORMATION

I.V. Dyachenko, ORCID: https://orcid.org/0000-0001-7255-3446

V.D. Dyachenko, ORCID: https://orcid.org/0000-0002-0993-4091

V.N. Khrustalev, ORCID: https://orcid.org/0000-0001-8806-2975

V.G. Nenajdenko, ORCID: https://orcid.org/0000-0001-9162-5169

FUNDING

This study was performed under financial support by the Russian Foundation for Basic Research (project no. 18-53-34002) and by the Ministry of Science and Higher Education of the Russian Federation (project no. 075-03-2020-223, FSSF-2020-0017).

CONFLICT OF INTEREST

The authors declare the absence of conflict of interest.

REFERENCES

1. Nesaragi, A.R., Kamble, R.R., Hoolageri, S.R., Mavazzan, A., Madar, S.F., Anand, A., and Joshi, S.D., *Appl. Organomet. Chem*., 2021, vol. 36, article ID e6469. https://doi.org/10.1002/aoc.6469
2. Eghtedari, M., Sarrafi, Y., Nadri, H., Mahdavi, M., Moradi, A., Moghadam, F.H., Emami, S., Firoozpour, L., Asadipour, A., Sabzevari, O., and Foroumadi, A., *Eur. J. Med. Chem*., 2017, vol. 128, p. 237. https://doi.org/10.1016/j.ejmech.2017.01.042
3. Abd-El-Aziz, A.S., El-Agrody, A.M., Bedair, A.H., Corkery, T.C., and Ata, A., *Heterocycles*, 2004, vol. 63, p. 1793. https://doi.org/10.3987/COM-04-10089
4. Mishriky, N., Girgis, A.S., Asaad, F.M., Ibrahim, Y.A., Sobien, U.I., and Fawzy, N.G., *Boll. Chim. Farm*., 2001, vol. 140, p. 129.
5. Recio, R., Vengut-Climent, E., Mouillac, B., Orcel, H., López-Lázaro, M., Calderón-Montaño, J.M., Álvarez, E., Khiar, N., and Fernández, I., *Eur. J. Med. Chem*., 2017, vol. 138, p. 644. https://doi.org/10.1016/j.ejmech.2017.06.056
6. Wardakhan, W.W., Samir, E.M., and El-Arab, E.E., *Bull. Chem. Soc. Ethiop*., 2018, vol. 32, p. 259. https://doi.org/10.4314/bcse.v32i2.7
7. Azzam, R.A. and Mohareb, R.M., *Chem. Pharm. Bull*., 2015, vol. 63, p. 1055. https://doi.org/ 10.1248/cpb.c15-00685
8. Marco-Contelles, J., León, R., López, M.G., García, A.G., and Villarroya, M., *Eur. J. Med. Chem*., 2006, vol. 41, p. 1464. https://doi.org/10.1016/j.ejmech.2006.06.016
9. Thanh, N.D., Hai, D.S., Ha, N.T.T., Tung, D.T., Le, C.T., Van, H.T.K., Toan, V.N., Toan, D.N., and Dang, L.H., *Bioorg. Med. Chem. Lett*., 2019, vol. 29, p. 164. https://doi.org/ 10.1016/j.bmcl.2018.12.009
10. Saundane, A.R., Vijaykumar, K., and Vaijinath, A.V., *Bioorg. Med. Chem. Lett*., 2013, vol. 23, p. 1978. https://doi.org/10.1016/j.bmcl.2013.02.036
11. Boulebd, H., Ismaili, L., Bartolini, M., Bouraiou, A., Andrisano, V., Martin, H., Bonet, A., Moraleda, I., Iriepa, I., Chioua, M., Belfaitah, A., and Marco-Contelles, J., *Molecules*, 2016, vol. *21, no.* 4, article no. 400. https://doi.org/10.3390/molecules21040400
12. Al-Omar, M.A., Youssef, K.M., El-Sherbeny, M.A., Awadalla, S.A.A., and El-Subbagh, H.I., *Arch. Pharm*., 2005, vol. 338, p. 175. https://doi.org/10.1002/ardp.200400953
13. AbdEl-Azim, M.H.M., Aziz, M.A., Mounier, S.M., EL-Farargy, A.F., and Shehab, W.S., *Arch. Pharm*., 2020, vol. 353, article ID 2000084. https://doi.org/10.1002/ardp.202000084
14. Mahmoud, N.F.H. and Balamon, M.G., *J. Heterocycl. Chem*., 2020, vol. 57, p. 3056. https://doi.org/10.1002/jhet.4011
15. Ismail, M.M.F., Khalifa, N.M., Fahmy, H.H., Nossier, E.S., and Abdulla, M.M., *J. Heterocycl. Chem*., 2014, vol. 51, p. 450. https://doi.org/10.1002/jhet.1757
16. Dyachenko, V.D. and Pugach, Yu.Yu., *Russ. J. Gen. Chem*., 2013, vol. 83, p. 979. https://doi.org/10.1134/S1070363213050162
17. Dyachenko, V.D. and Rusanov, E.B., *Chem. Heterocycl. Compd*., 2004, vol. 40, p. 231. https://doi.org/10.1023/B:COHC.0000027898.06493.c5

18. Dyachenko, V.D. and Rusanov, E.B., *Russ. J. Org. Chem*., 2006, vol. 42, p. 1374. https://doi.org/10.1134/S1070428006090211
19. Dyachenko, V.D. and Chernega, A.N., *Russ. J. Gen. Chem*., 2005, vol. 75, p. 952. https://doi.org/10.1007/s11176-005-0351-6
20. Dyachenko, V.D. and Pugach, Yu.Yu., *Russ. J. Gen. Chem*., 2012, vol. 82, p. 921. https://doi.org/10.1134/S1070363212050209
21. Suáreza, M., Salfrán, E., Verdecia, Y., Ochoa, E., Alba, L., Martín, N., Martínez, R., Quinteiro, M., Seoane, C., Novoa, H., Blaton, N., Peeters, O.M., and Ranter, C., *Tetrahedron*, 2002, vol. 58, no. 5, p. 953. https://doi.org/10.1016/S0040-4020(01)01189-9
22. Dyachenko, V.D. and Chernega, A.N., *Russ. J. Org. Chem*., 2006, vol. 42, p. 567. https://doi.org/10.1134/S1070428006040142
23. Dyachenko, V.D., *Russ. J. Gen. Chem*., 2004, vol. 74, p. 1463. https://doi.org/10.1007/s11176-005-0035-2
24. Andin, A.N., *Russ. J. Org. Chem*., 2018, vol. 53, p. 804. https://doi.org/10.1134/S1070428018050251
25. Chennapuram, M., Emmadi, N.R., Bingi, C., Nanubolu, J.B., and Atmakur, K., *Green Chem*., 2014, vol. 16, p. 3237. https://doi.org/10.1039/C4GC00388H
26. Dyachenko, V.D., *Russ. J. Gen. Chem*., 2005, vol. 75, p. 1537. https://doi.org/10.1007/s11176-005-0463-z
27. Bruker SAINT, Madison, WI: Bruker AXS, 2013.
28. Krause, L., Herbst-Irmer, R., Sheldrick, G.M., and Stalke, D., *J. Appl. Crystallogr*., 2015, vol. 48, p. 3. https://doi.org/10.1107/S1600576714022985
29. Battye, T.G.G., Kontogiannis, L., Johnson, O., Powell, H.R., and Leslie, A.G.W., *Acta Crystallogr., Sect. D*, 2011, vol. 67, p. 271. https://doi.org/10.1107/S0907444910048675
30. Evans, P.R., *Acta Crystallogr., Sect. D*, 2006, vol. 62, p. 72. https://doi.org/10.1107/S0907444905036693
31. Sheldrick, G.M., *Acta Crystallogr., Sect. C*, 2015, vol. 71, p. 3. https://doi.org/10.1107/S2053229614024218